Vol. 14, No. 2 (2025): 391 - 403 http://dx.doi.org/10.23960/jtep-l.v14i2.391-403

JURNAL TEKNIK PERTANIAN LAMPUNG

ISSN 2302-559X (print) / 2549-0818 (online)
Journal homepage : https://jurnal.fp.unila.ac.id/index.php/JTP

Optimization of Suction Channel System on Vacuum-Type Soybean Seed Metering System Powered by Hand Tractor

Adhiasta Faris Setiabudi[1], Wawan Hermawan[1,✉], Radite Praeko Agus Setiawan[1]

[1] Department of Mechanical and Biosystem Engineering, Faculty of Agricultural Technology, IPB University, Bogor, INDONESIA.

Article History:

Received : 25 July 2024
Revised : 29 November 2024
Accepted : 10 December 2024

Keywords:

CFD,
Metering device,
Optimization,
Pneumatic,
Soybean.

Corresponding Author:
✉ w_hermawan@apps.ipb.ac.id
(Wawan Hermawan)

ABSTRACT

A vacuum-type soybean seeder powered by hand tractor for Indonesia's local soybean has been developed to overcome soybean low productivity. The developed machine still has a weakness in the context of the suction channel system. This research was conducted to optimize the suction channel system efficiency, suction performance for bigger type of seed variety, and suction effect uniformity on all metering device. The research step consisted of seed characteristic measurement for two Indonesia's common local soybean seed variety (Anjasmoro and Grobogan), suction channel system modification and analysis, and validation based on computational fluid dynamic (CFD). The result in this research are proposed 3-types of optimized model with final selection of 1-type of model, namely Branch model. The values produced by the optimized model compared to existing model respectively 3.393 kPa (CV 0.10%) and 3.112 kPa (CV 1.54%) for negative pressure, 14.39 m/s (CV 4.11%) and 9.08 m/s (3.44%) for suction velocity, as well as 117.342 Pa and 118.147 Pa for total pressure-loss. The required value for Anjasmoro and Grobogan seed variety respectively 3.094 kPa and 3.358 kPa for negative pressure pressure, as well as 10.22 m/s and 10.03 m/s for suction velocity. Hence, the selected optimized model is more efficient, uniform, and can accommodate required negative pressure pressure and suction velocity for both Anjasmoro and Grobogan, while the existing model can only accommodate Anjasmoro.

1. INTRODUCTION

Soybeans are one of Indonesia's staple food commodities that has increase of demand in a recent years. Sagita *et al*. (2018) developed a soybean seed planter (4-unit per implement) integrated with fertilizer powered by a hand tractor to replace the conventional seed planting process. The development was based on Hermawan *et al*. (2016) design that used two-wheel hand tractor instead of four-wheel tractor due to Indonesian farmer preferences. Vacuum-type or pneumatic system was chosen for seed metering mechanism since Indonesia local seed has dramatic variation of dimension. Hence, conventional metering device or non-pneumatic mechanism will only produce inconsistency, doubling, skipping, or damaged seed planting (Hermawan *et al*., 2016).

The existing soybean seed planter developed by Sagita *et al*. (2018) still has several issues that can be optimized in terms of seed metering performance by the vacuum-type metering device (MD). The suction channel system was not considered deeply, resulting in a relatively high pressure drop and low uniform suction effect on all of the four MD units. This low uniform suction affect cause some of the MD producing a high pressure resulting multiplication planting and some of the MD producing low pressure resulting miss planting. Configurating higher suction-blower suction speed is less of a primary option because technically the suction-blower speed follows the engine rotation, which is often changed by the operator to adjust the machine's performance to field conditions.

The objective of this study was to optimize the suction channel system in Sagita *et al*. (2018) design to enhance seed metering performance. Suction variable in Indonesia local soybean varieties (Anjasmoro & Grobogan) will be measure for basis of design requirement.

2. MATERIALS AND METHODS

2.1. Suction-related Measurement for Soybean Seed

Seed characteristics were measured to identify physical differences between seed varieties that could influence the vacuum-type seed metering performance. The parameters of interest included seed suction pressure or alternatively referred as negative pressure ΔP_s (kPa) and seed terminal velocity or alternatively referred as seed suction velocity, v_s (m/s). The seeds used in this experiment were of the Anjasmoro and Grobogan varieties. The physical dimensions and mass characteristics of the Grobogoan variety seeds are relatively larger than the Anjasmoro variety, both in length, width, and thickness (Kurniawardani *et al*., 2023). Thus, the contrast difference from the seed is considered for seed metering performance study.

The requirement negative pressure of soybean seed was measured using a mathematical model developed by Karayel *et al*. (2004), as shown in Equation 1.

$$\Delta P_S = 1 + 0.72 m_{1000}^{0.27} + 2.09 \times 10^{-3} A_S^{-0.02} - 0.01 \Psi_S + 0.37 \times 10^{-3} \rho_S \quad (1)$$

This mathematical model has a root mean square error (RMSE) value of 2.74×10^{-2} and modeling efficiency of 99%. The model pertains to seed characteristics with parameters including seed mass of 1000 seeds (m_{1000} [g]), seed projected area A_S (mm^2), seed sphericity ψ_S (%), and seed bulk density ρ_S (kg/m^3). Values of A_s and ψ_s require seed dimension data obtained through measurements along three seed axes, namely: length L (mm), width W (mm), and thickness T (mm). After dimension measurements, seed mass was determined using a digital scale. Sampling of seed dimensions and mass was conducted with 100 seeds for each variety.

The variable of terminal seed velocity, was directly measured using a vertical pipe method that propelled seeds upwards using an air blower. The measurement method for terminal seed velocity follows the approach outlined by Matouk *et al*. (2005), utilizing blower to push seed sample in transparent vertical tube. The calculation of seed terminal velocity is based on the number of seeds blown out at a certain air speed. Twenty seeds are randomly selected and placed on a plastic net, a mesh layer that can hold the seeds but still allows the airflow to pass through. At a certain blower speed, the airflow created by the blower will push the seeds from below the plastic net until they are lifted and exit the transparent tube. The terminal velocity of the seeds using Matouk *et al*. (2005) method is calculated using Equation 2:

$$v_S = \frac{Q_1 v_{S1} + Q_2 v_{S2} + \cdots + Q_n v_{Sn}}{Q_1 + Q_2 + \cdots + Q_n} \quad (2)$$

In this equation, Q_n represents the number of seeds that successfully exit the transparent tube at a specific blower speed configuration v_S (m/s). The test is repeated five times for each set of 20 seed samples for each variety. The smaller the changes in air speed applied to the seeds, the more accurate the terminal velocity (Equation 2) will be.

2.2. Alternatives Creation of Suction Channel System

Three alternative designs for suction channel system are proposed. Components that could potentially be modified to significantly enhance suction performance include the air distributor design, layout, and air distribution method. The main-channels are divided into two-type: the primary channel (from suction-blower suction port to air distributor) and the secondary channels (from air distributor to metering device discharge port). The existing suction channel system scheme by Sagita *et al*. (2018) is illustrated in Figure 1A. The current design of the air distributor needs to be replaced with a more symmetric shape to ensure even air distribution. The most symmetric method of air distribution can be implemented gradually, dividing it not all at once into 4 units, but first into 2 channel, which are then divided into 2

more channel each for 4 units. This distribution method resembles a branching structure (namely the Branch model) as shown in Figure 1B. This type of model required more air distributors unit in the system. Practically, this model can be simplified so that there is only 1 air distributor, and the distance of each secondary channel to the air distributor remains the same. The schematic of this model resembles a fork (namely the Fork model), as shown in Figure 1C. Also, there are two-type of concept in term of air distributor position: positioning the air distributor in front (similar to the existing, Branch, and Fork model) or behind. The air distributor model positioned behind takes on a squid-like shape (namely the Squid model), as shown in Figure 1D. Positioning the air distributor behind results in longer primary channels than the secondary channels compared to other model. Thus, lowering the friction factor by flowing frequently in the primary/larger channel (Nur *et al*., 2019). Although the lengths of the secondary channels in the Squid model are not identical, the differences in length are relatively insignificant.

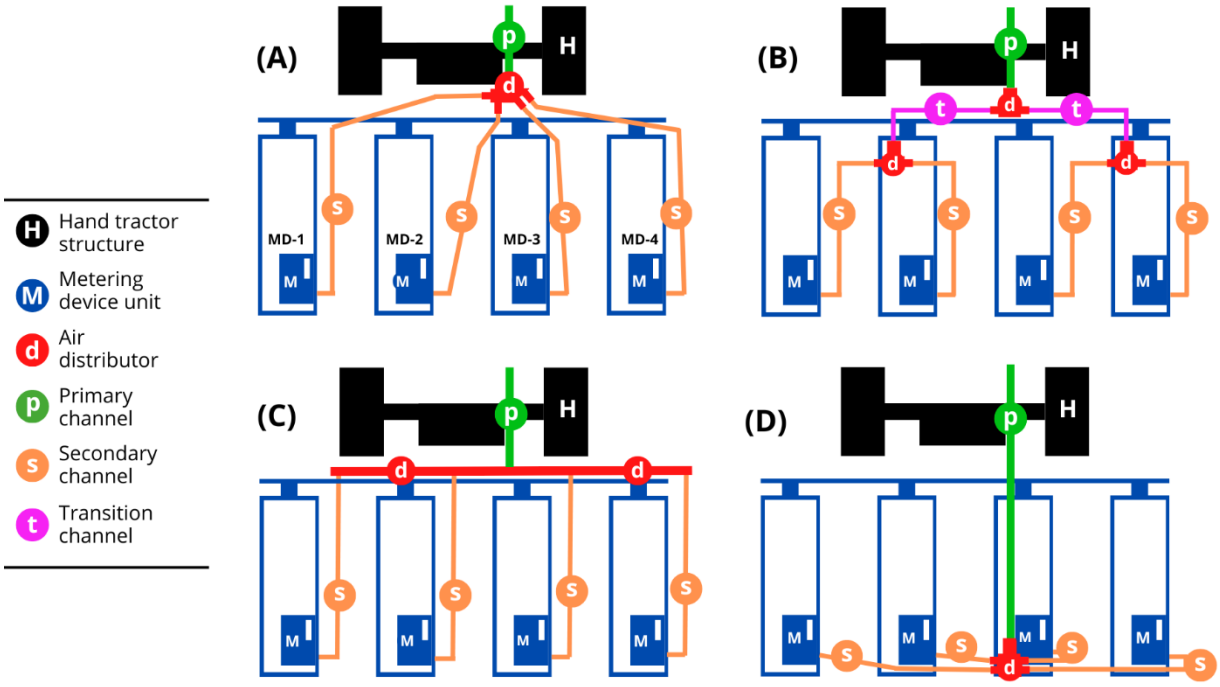

Figure 1. Schematic for suction channel system alternative: A (existing model); B (Branch model); C (Fork model); D (Squid model)

Each alternative design has its own potential strengths and weaknesses. These aspects are too biased to be considered non-parametrically. Alternative models also need to take into account commercial aspects and the level of complexity for manufacturing activities. The potential drawbacks and advantages of each model need to be validated to determine the alternative with the highest performance advantages in terms of seed metering performance, channel efficiency, suction effects uniformity, and require component complexity.

2.3. Computational Fluid Dynamics (CFD) Configuration

The results of modifying the suction channel system were validated using computational fluid dynamics (CFD). Configuration used for the simulation was based on internal flow. CFD parameters were determined based on direct measurements by Sagita *et al*. (2018), including the use of air as the fluid at 30 degrees Celsius and the suction-blower impeller rotation speed set at 6000 RPM. The impeller was configured using a local region type sliding setup (Aldio *et al*., 2023). A no-slip configuration was used to approximate the realistic fluid characteristics near the pipe walls (Lamsal, 2023), considering small channel diameter (1 in and 2 in). The best material for fluid transportation using pipes refers to research by Chakraborty *et al*. (2016), namely polyvinyl chloride (PVC), with absolute roughness value

(ε_c) used is 0.0015 micrometers (Uribe *et al*., 2015; da Silva *et al*., 2022). The boundary condition configuration included only ambient environmental conditions (atmospheric pressure) applied at all inlets/outlets.

The variables acquired from the simulation results (referred to as goals plot) included model negative pressure and model suction velocity. Each variable is acquired at specific measurement points: the suction port of the suction-blower, the suction port of the primary hose, and the discharge port of all of four MD unit. The model negative pressure ΔP_{mod} (kPa) is determined by calculating the difference between atmospheric pressure (101.325 kPa) and the absolute pressure obtained from the simulation. Model suction velocity v_{mod} (m/s) is the average velocity over a specific cross-sectional area obtained from the simulation result. The v_{mod} need to be converted into suction velocity per seed hole (v_{SH}) with continuity equation. Suction effect uniformity then can be calculated based on coefficient of variation (CV) for both model's negative pressure and model's suction velocity.

Calibration of the mesh-level in the CFD simulation are necessary for better result. Mesh-levels, as recommended by the software or auto-mesh generated, range from level 1 (coarse mesh) to level 7 (fine mesh). Higher mesh-levels yield better accuracy but also result in longer simulation durations (Pérez & Vakkilainen, 2018). Convergence testing is essential to determine the appropriate mesh-level, that involves conducting simulations repeatedly with different mesh-levels (Hizir *et al*., 2018), starting from the coarsest mesh-level. Convergence testing is beneficial for minimizing simulation duration while seeking optimal simulation accuracy. It is performed on the existing model due to its higher complexity compared to other alternatives, and because direct measurement data is available from by Sagita *et al*. (2018).

2.4. Pressure-Loss Analysis

Channel efficiency is calculated based on the pressure-loss factor. There are two causes of pressure-loss in the channel system, namely friction-loss ΔP_F (Pa) due to fluid friction against the wall and local-loss ΔP_L (Pa) due to the influence of local components on the channel system. The total pressure-loss ΔP_{loss} (Pa) is expressed as:

$$\Delta P_{loss} = \sum_{i=1}^{n} \Delta P_{F_i} + \Delta P_{L_i} \tag{3}$$

The type of flow that occurs (laminar, transition, or turbulent) needs to be known first by calculating the Reynolds number *Re* (LaNasa & Upp, 2014) in the form of:

$$Re = \frac{\rho D_C \bar{v}}{\mu} = \frac{D_C \bar{v}}{\nu} \tag{4}$$

Based on the Touloukian (1970), air properties at a temperature of 30°C include air density (ρ) of 1.164 kg/m^3, dynamic viscosity (μ) of 18.72(10^{-6}) Pa·s, and kinematic viscosity (V) of 16.08(10^{-6}) m^2/s. The average air speed value ($\bar{v}$) is obtained from the simulation results at a point with a certain channel diameter (D_C). The form of flow that occurs at a point is laminar flow if $Re < 2100$, transition flow if $2100 < Re < 4000$, and turbulent flow if $Re > 4000$. The pressure-loss in a long channel L_C (m) due to friction-loss follows the Darcy-Weisbach equation:

$$\Delta P_F = f_D \frac{\rho L_C \bar{v}^2}{2 D_C} \tag{5}$$

The Darcy friction coefficient f_D follows the flow conditions that occur. The pressure-loss in the channel due to local-loss follows the Darcy-Weisbach equation:

$$\Delta P_L = K_L \frac{\rho_{air} \bar{v}^2}{2} \tag{6}$$

The loss coefficient (K_L) is influenced by type and size fitting channel, such as diameter, angle of the elbow, number of paths tee, the inflow direction through reducer, and others.

2.5. Alternative Assessment and Selection Method

The four alternative models of the suction channel system, consisting of one existing model and three proposed optimization models, need to be selected for further research. Six criteria are considered in the model selection

process. These six criteria are categorized into two types: mandatory criteria and additional criteria. Suction performance criteria (negative pressure and suction speed) are mandatory as they determine whether the model's performance meets the required seed characteristics. The remaining four criteria are additional considerations, each with its own weigh-point. The suction effects uniformity carries the highest priority due to its importance in ensuring consistent dispensing performance across the four MD units. The number of components criterion has the lowest weight as it does not directly affect the seed dispensing performance. The criteria for selecting the alternative suction channel system models are presented in Table 1.

Table 1. Technical requirement for model scoring

Criteria	Weight Value	Target
$\Delta P_{mod} > \Delta P_S$ $\bar{v}_{SH} > v_S$	Mandatory	Achieved across all four MD
CV for ΔP_{mod}	35%	Lowest CV value
CV for $\bar{v}_{SH}$	35%	Lowest CV value
Total ΔP_{loss}	20%	Lowest total value
Total component used	10%	Lowest total value

The four additional criteria have different forms of values, therefore, they need to be standardized using a scaled comparison. This method involves transforming a criterion value (x_n) into a new value within a specified range (y_n). The planned scale is 10, so all criterion values $y_n$will be within the range of 0-10. The four additional criteria share the same target, which is the lowest value. Therefore, this scaled comparison method relies on the smallest value within the same criteria (x_{1-4}) through the following formulation:

$$y_n(x_n) = \frac{min\{x_{1-4}\}}{x_n} \times 10 \quad (7)$$

3. RESULTS AND DISCUSSION

3.1. Soybean Seeds Characterization

The measured characteristics of soybean seeds are summarized in Table 2. The soybean seed characteristics of Anjasmoro and Grobogan varieties exhibit several differences that can influence their interaction with fluids. The physical dimensions and mass of Grobogan seeds are relatively larger compared to Anjasmoro seeds, in terms of length, width, and thickness. This finding aligns with Kurniawardani *et al*. (2023), who noted a trend towards larger seed size in Grobogan compared to other varieties. Consequently, Grobogan seeds have a larger surface area than Anjasmoro seeds. The bulk density of Grobogan seeds tends to be smaller than that of Anjasmoro seeds, likely due to smaller seeds leaving fewer air cavities between seed stacks, and vice versa. On the other hand, sphericity does not show significant differences between the two varieties. Terminal seed velocities measured for both varieties do not differ significantly, but Anjasmoro tends to have higher values. Technically, the larger surface area of Grobogan seeds

Table 2. Soybean seed characterization measurement

Parameter	Unit	Anjasmoro	Grobogan
Length dimension (L)	mm	7.91 ± 0.70	8.32 ± 0.66
Width dimension (W)	mm	6.18 ± 0.49	6.63 ± 0.51
Thick dimension (T)	mm	4.77 ± 0.47	5.03 ± 0.50
Single seed mass (m_S)	g	0.158 ± 0.038	0.199 ± 0.042
Projected area (A_S)	mm^2	103.46 ± 16.39	116.19 ± 16.21
Bulk density (ρ_S)	g/cm^3	0.910 ± 0.003	0.854 ± 0.007
Sphericity (ψ_S)	%	77.90 ± 3.77	78.49 ± 4.61
Terminal velocity (v_S)	m/s	10.22 ± 0.54	10.03 ± 0.60
Required negative pressure (ΔP_S)	kPa	3.094 ± 0.131	3.358 ± 0.119

provides more contact for air to exert pressure. The negative pressure requirements for soybean seeds refer to the model by Karayel *et al*. (2004), which indicates higher negative pressure requirements for Grobogan compared to Anjasmoro. Negative pressure variables are inversely related to suction velocity variables, explaining the fundamental fluid power needed to suction seeds. Resulted negative pressure for both Anjasmoro and Grobogan is not significantly different from that recommended by Karayel *et al*. (2022) and Ismail (2014), which is 3 kPa.

3.2. Detailed Design of Suction Channel System

The concept of the proposed alternative suction channel system scheme needs detailed design to be used as a model in CFD simulations. The alternative design considers the availability of commercial materials such as standard pipe sizes and pipe fittings (elbows, reducers, and tees) in inches. Detailed designs of each alternative suction system model are illustrated in Figure 2.

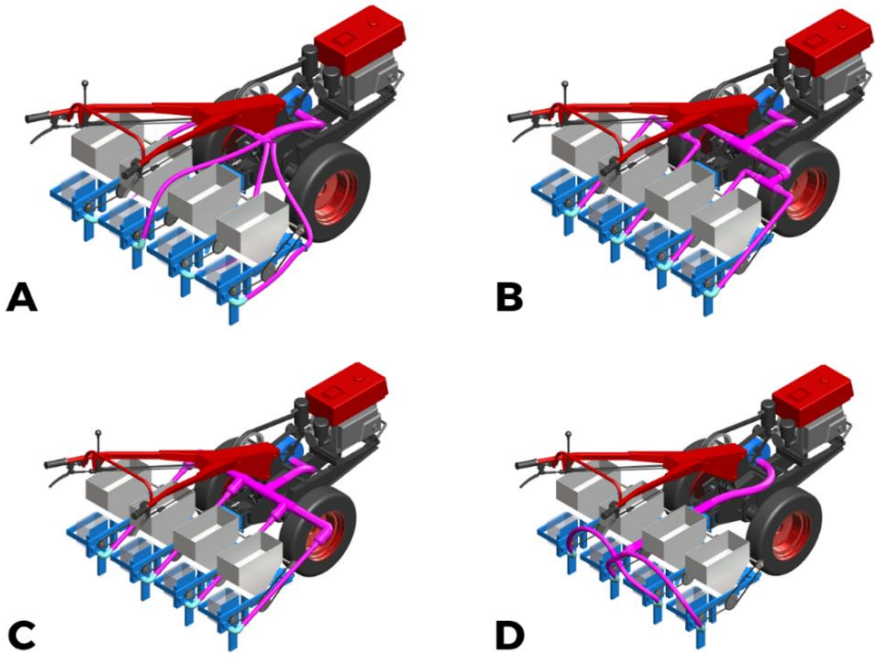

Figure 2. Detailed design of suction channel system: A (existing model); B (Branch model); C (Fork model); D (Squid model)

The detailed design of the alternative models differs in the number and type of channels and fittings due to adjustments to the proposed schematic configurations. The existing model utilizes four flexible hoses for the secondary channels. A drawback of this concept is the significant length variation among the four channels and the overall longest total channel length compared to other models. Increased channel length leads to a greater distance the air must travel, thereby increasing the pressure drop. Surprisingly, the Fork model results in a longer total channel length compared to the Branch model, despite the Fork model's purpose being to simplify the Branch model. However, the Fork model is simpler than the Branch model in terms of fitting requirements or components causing local-loss. Conversely, the Squid model features the shortest total channel length among the models. In addition to having the shortest total channel length, the Squid model has the fewest local-loss components compared to the Fork and Branch models. On the other hand, a limitation of the Squid model is its continued reliance on flexible hoses, similar to the existing model, although its channel length is shorter.

The elements that influence the efficiency of the channel are the number of local-loss components used in the system and the length of the suction channel. The term "local-loss components" refers to components that contribute to local-loss value (i.e. flexible hoses has potential to cause local-loss from its bends, despiet they are not consider as fitting component). List of local-loss component detailed in Table 3, and the suction channel lengths in Table 4.

Table 3. List of local-loss component on model

Item No.	Local-loss Component		K_L	Quantity			
				Existing	Branch	Fork	Squid
1	Elbow	90deg 1.0 in	0.23	4	8	4	4
2	Elbow	90deg 1.5 in	0.23	-	2	-	-
3	Elbow	90deg 2.0 in	0.23	-	-	2	-
4	Reducer	Conc. 1.0-1.5 in	0.41	-	4	-	-
5	Reducer	Conc. 1.5-2.0 in	0.15	-	2	-	-
6	Reducer	Conc. 1.0-2.0 in	0.70	-	-	4	1
7	Tee	3way-equal 1.0 in	0.27	-	-	-	-
8	Tee	3way-equal 1.5 in	0.27	-	2	-	-
9	Tee	3way-equal 2.0 in	0.27	-	1	3	-
10	Tee	5way-cross 1.0 in	0.68	-	-	-	1
11	Tee	Custom	0.68	1	-	-	-
12	Flexible hose curvature		0.5	4	-	-	4

Table 4. Suction channel length on model

Type of Channel	Channel Length (L_C) [mm]			
	Existing	Branch	Fork	Squid
Primary	685	685	685	1510
Secondary-1	1320	655	990	640
Secondary-2	985	655	680	200
Secondary-3	1106	655	680	340
Secondary-4	1273	655	990	830
Transitional-1	-	165	-	-
Transitional-2	-	165	-	-
Total Length	5369	3635	4025	3520

3.3. Simulation Configuration Validation

The convergence test of the simulation was conducted with reference to negative pressure and suction velocity parameters obtained at six measurement points. Regarding negative pressure parameter, convergence indication was observed (see Figure 3) from mesh-level 5 to mesh-level 6. However, for the fluid velocity parameter, convergence was noted from mesh-level 6 to mesh-level 7. Therefore, the mesh-level utilized in the simulation model is mesh-level 7. The comparison between the simulation results at mesh-level 7 and the existing data can be seen in Table 5, with error calculations based on Mean Absolute Percentage Error (MAPE).

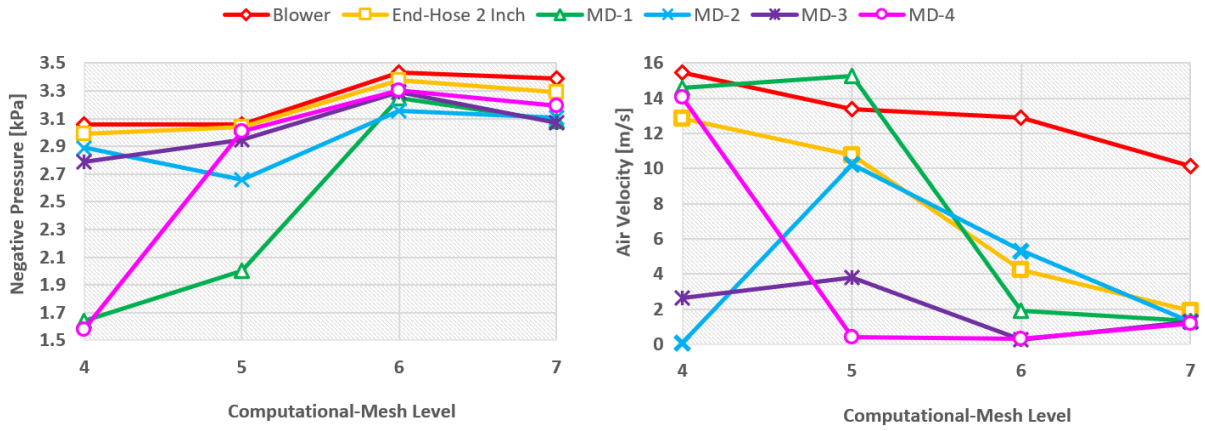

Figure 3. Convergence test on difference computational-mesh level

Table 5. Output deviation of CFD mesh-level 7 compared to actual value on existing model

Point of Measurement	Unit	Negative Pressure (ΔP_{mod})		MAPE
		Actual	CFD	
Suction Port Suction-Blower	kPa	N/A	3.388	-
Suction Port Primary Channel	kPa	3.187	3.289	5.96%
Discharge Port MD-1	kPa	2.732	3.080	12.75%
Discharge Port MD-2	kPa	2.677	3.108	16.11%
Discharge Port MD-3	kPa	2.732	3.070	12.36%
Discharge Port MD-4	kPa	2.815	3.191	13.35%
Average MAPE value				11.56%

The MAPE value indicates that mesh-level 7 can produce deviations of actual values from simulation results that are still below 15%. This suggests that the configuration and simulation model can proceed confidently. The comparison is specifically conducted for negative pressure parameters, as there are no actual values available for suction velocity parameters according to Sagita *et al.* (2018).

3.4. Performance Analysis on Suction Channel System

The simulation was conducted on a full-scale, end-to-end basis due to significant differences observed when simulations are performed partially. This phenomenon arises from two factors: the suction-blower mechanism and air restriction. The suction-blower mechanism (centrifugal pump) is a non-positive displacement pump, which transfers fluid without relying on seals or valves. Unlike positive displacement pumps, which force flow from the inlet to the outlet without backflow effects, non-positive displacement pumps cannot prevent backflow. Research by Sun *et al.* (2023) found that increasing the impeller rotation speed of a centrifugal blower beyond an optimal point only increases energy loss and noise levels. Conversely, excessively small seed holes lead to air restriction, which can exacerbate backflow effects. At any given time, the amount of air entering the channel through the seed hole cannot accommodate the volume of air being expelled by the blower. This results in a "spring effect" on the air within the channel, potentially causing air to be pulled back by the blower, thereby reducing the negative pressure. The numerical CFD simulation results for the four alternatives are detailed in Table 6.

The negative pressure generated by each model must be sufficient to meet the seed suction requirements. Based on the analysis, the seed negative pressure requirements are 3.094 kPa (Anjasmoro) and 3.358 kPa (Grobogan). Existing models are inadequate for meeting the negative pressure requirements for the Grobogan variety, as the design by Sagita *et al.* (2018) was developed specifically for the Anjasmoro variety. The Squid model can also only accommodate the Anjasmoro variety. In contrast, the Branch and Fork models can accommodate both the Anjasmoro

Table 6. Parametric result based on CFD

P_{mod} Acquisition Point	Unit	Existing	Branch	Fork	Squid
Negative Pressure (ΔP_{mod})					
Suction Port Suction-Blower	kPa	3.388	3.702	3.340	3.185
Suction Port Primary Channel	kPa	3.289	3.633	3.364	3.281
Discharge Port MD-1	kPa	3.080	3.388	3.428	3.329
Discharge Port MD-2	kPa	3.108	3.397	3.421	3.297
Discharge Port MD-3	kPa	3.070	3.391	3.431	3.299
Discharge Port MD-4	kPa	3.191	3.396	3.419	3.323
Suction Velocity ($\bar{v}_{mod}$)					
Suction Port Suction-Blower	m/s	10.12	11.30	11.20	9.18
Suction Port Primary Channel	m/s	1.92	2.30	2.28	2.66
Discharge Port MD-1	m/s	1.31	1.93	1.52	2.10
Discharge Port MD-2	m/s	1.27	2.08	1.72	2.08
Discharge Port MD-3	m/s	1.30	2.10	1.73	2.13
Discharge Port MD-4	m/s	1.20	1.92	1.52	2.15

and Grobogan varieties. The Branch model exhibits the highest negative pressure in the secondary channels compared to the other models. This is due to the gradual transition in channel size. Unlike other models, the Branch model does not directly connect the 2-inch primary channel to four 1-inch secondary channels but rather divides it into two 1.5-inch transitional channels first. This facilitates the convergence of the suction flow toward the suction-blower. Unlike the other models, the Fork model has a slight difference from the Branch model, namely the absence of a hose size transition to reduce the channel length. As such, a 1-inch secondary hose is directly connected to the other secondary hoses via a 2-inch tee.

The acquisition points for suction velocity data in Table 6, specifically at the discharge ports of the MD units, need to be converted to the area of the seed hole using the fluid continuity equation (Mukilan & Vivek, 2023). The area of the seed hole is calculated based on the diameter of the air hole formed in the seed hole (planned at 3 mm), assumed efficiency of 90%, and the number of effective seed holes. There are two conditions for the seed holes during operation: seed holes affected by suction (referred to as active seed holes) and seed holes not affected by suction for releasing the seeds being distributed. The planned number of seed holes per unit in the study is 12 seed holes (9 active seed holes with 3 cut-off seed hole). The velocity achieved at each active seed hole can be seen in Table 7.

The suction velocity at each seed hole needs to exceed the terminal velocity of the seeds in order to facilitate seed suction. The terminal velocities for the seeds are 10.22 m/s for the Anjasmoro variety and 10.03 m/s for the Grobogan variety. The existing model is unable to achieve the minimum suction velocity requirement. Conversely, all optimized models—the Branch, Fork, and Squid models—are capable of meeting the minimum suction velocity threshold.

Table 7. Suction velocity in single active seed hole

Unit MD	Seed Hole Suction Velocity ($\bar{v}_{SH}$) [m/s]			
	Existing	Branch	Fork	Squid
MD-1	9.36	13.81	10.92	15.07
MD-2	9.07	14.93	12.34	14.91
MD-3	9.31	15.02	12.37	15.26
MD-4	8.57	13.78	10.90	15.41

Table 8. Non-uniformity suction effect based on coefficient of variation

Parameter	Existing	Branch	Fork	Squid
Negative Pressure (ΔP_{mod})	1.54%	0.10%	0.15%	0.43%
Suction Velocity ($\bar{v}_{SH}$)	3.44%	4.11%	6.19%	1.26%

The uniformity of suction effects across the four MD units is evaluated based on the CV. The CV values are derived from the ratio of the population standard deviation of the four MD unit parameters to their mean values. The Branch model demonstrates the best uniformity in negative pressure, followed by the Fork model, the Squid model, and the existing model. In contrast, the existing model shows the highest uniformity in suction velocity, followed by the Squid model, the Branch model, and the Fork model. The CV values for each model are presented in Table 8.

The CFD visualization results for the four alternatives can be seen in Figure 4 for the negative pressure distribution and Figure 5 for the suction speed distribution. The negative pressure is visualized using a color scale ranging from 3.0 to 3.8 kPa, where the lowest negative pressure is shown in blue and the highest in red. Meanwhile, the suction speed is visualized using a color scale ranging from 0-3 m/s, with red representing the highest suction speed and blue representing the lowest.

Channel efficiency is assessed from friction-loss and local-loss factors based on channel characteristics, using suction velocity values that obtain from CFD-based result. The flow type occurring in each channel for each model is resulted as turbulent. The friction factor (f_D) for turbulent flow can be obtained from the Moody diagram (Moody & Princeton, 1944). The total pressure-loss is analyzed for each suction channel across the four models. For all models except the Branch model, the suction channels are divided into five parts: one primary channel and four secondary channels. In the Branch model, there are two additional channels, which are transition channels. Based on total pressure

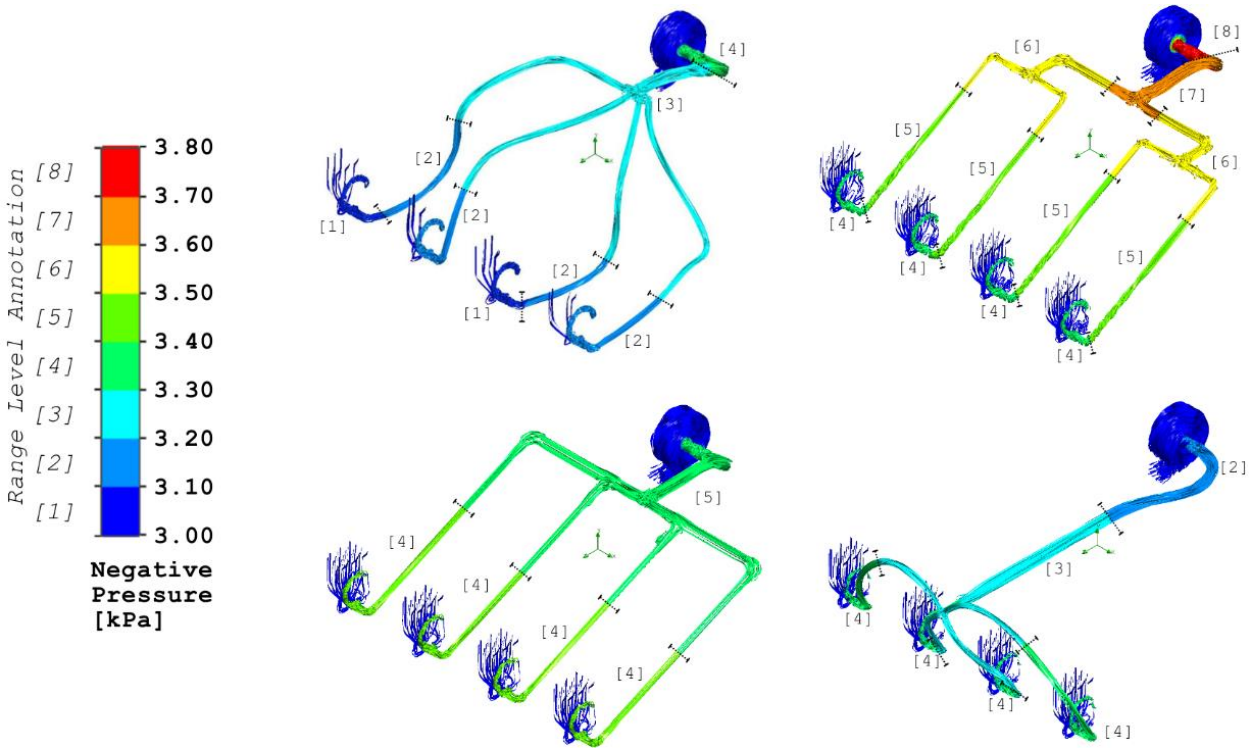

Figure 4. Visualization of negative pressure that occurs in the system (A: existing model; B: Branch model; C: Fork model; and D: Squid model)

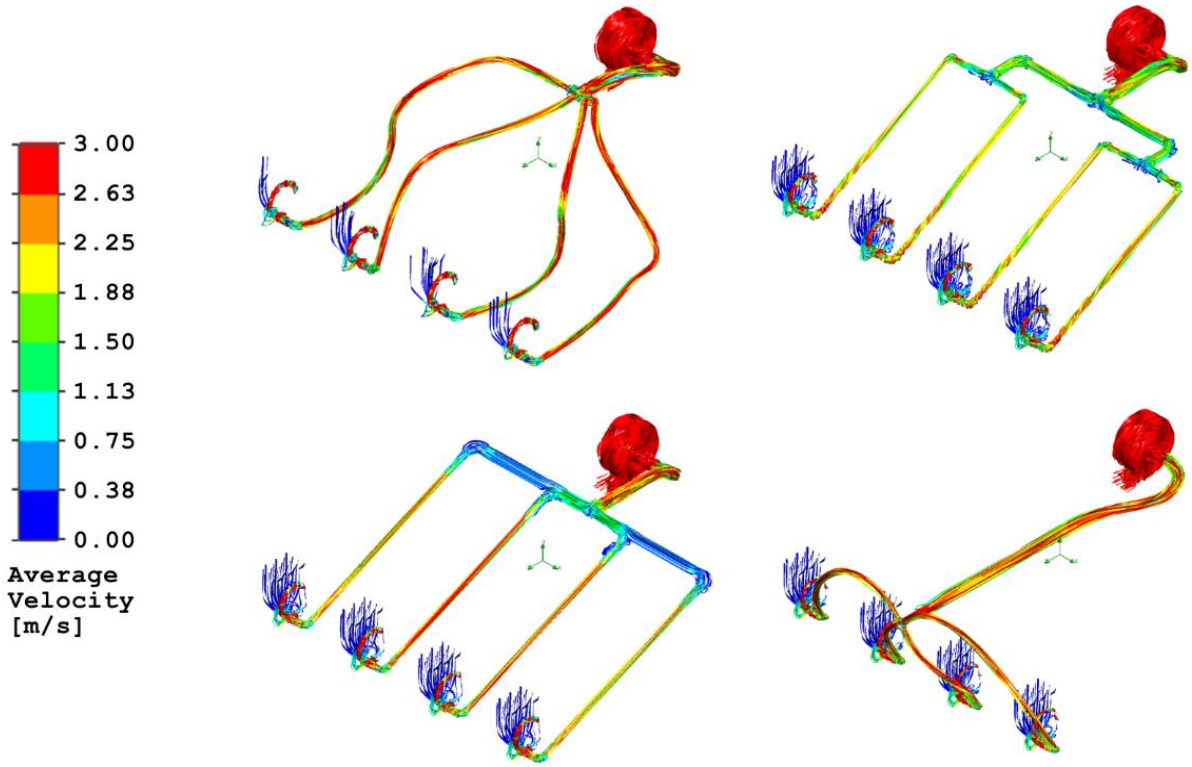

Figure 5. Visualization of suction velocity that occurs in the system (A: existing model; B: Branch model; C: Fork model; and D: Squid model)

loss, the Fork model exhibits the highest efficiency, followed by the Branch model, the existing model, and lastly the Squid model. For the largest friction-loss, the Squid model ranks highest, followed by the Branch model, the existing model, and the Fork model. In terms of local-loss, the Squid model also ranks highest, followed by the existing model, the Branch model, and the Fork model. This outcome aligns with the design objective of the Fork model, which aimed to simplify the Branch model in terms of both channels and fittings. The Squid model, which experiences the greatest pressure loss, does so because the impeller RPM of the suction-blower has exceeded the optimal point, resulting in increased pressure loss. This phenomenon is consistent with the findings of Sun *et al*. (2023). A reduction in the impeller RPM for the Squid model has the potential to improve efficiency, negative pressure, and suction velocity, warranting further investigation. The existing model demonstrates the lowest total pressure-loss in secondary channel-3. Sagita *et al*. (2018) reported the worst performance in channel-1 and channel-3. This discrepancy indicates that poor performance in MD-3 is not due to pressure-loss but rather to the air distributor design, which fails to distribute air uniformly across the four MD units. The detailed values of friction loss, local loss, and total pressure loss for each section of the channel in the four suction system models can be seen in Table 9.

Table 9. Pressure-loss calculation result

Channel	Existing	Branch	Fork	Squid
		Friction-loss (ΔP_F) [Pa]		
Primary	16.657	21.362	20.988	35.843
Secondary-1	16.985	13.323	14.115	16.731
Secondary-2	12.485	13.947	12.819	5.199
Secondary-3	14.194	13.999	12.834	8.952
Secondary-4	15.713	13.304	14.104	21.973
Transition-1	-	1.891	-	-
Transition -2	-	1.894	-	-
Total ΔP_F	76.034	79.721	74.859	88.697
		Local-loss (ΔP_L) [Pa]		
Primary	26.623	7.266	7.137	28.036
Secondary-1	4.434	5.391	7.772	9.873
Secondary-2	3.492	5.652	5.328	5.825
Secondary-3	2.653	5.674	5.334	5.903
Secondary-4	4.911	5.383	7.768	10.001
Transition-1	-	4.125	-	-
Transition -2	-	4.130	-	-
Total ΔP_L	42.113	37.622	33.339	59.638
		Pressure-loss (ΔP_{loss}) [Pa]		
Total ΔP_{loss}	118.147	117.342	108.198	148.335

Numerical result based on CFD simulation demonstrate various strengths and weaknesses for each model. The Branch model exhibits ideal negative pressure, suction speed, and good uniformity suction effect but is hindered by the large number of components required for assembly. The Fork model has advantages in achieving the highest negative pressure at the MD, the best channel efficiency, but suffers from very poor uniformity in suction speed. The Squid model excels in achieving the highest suction speed at the MD and requires the fewest components, but it has the worst channel efficiency, resulting in relatively low negative pressure at the MD. An alternative suction channel system model needs to be selected as a recommendation. The results of the mandatory criteria for the four suction channel system models can be seen in Table 10.

Based on the evaluation, the suction channel system models that meet the mandatory criteria are only the Branch model and the Fork model. Other considerations, the additional criteria, can be compared for each of the model. Using the scaled comparison method, the standardized values of the additional criteria can be reviewed based on their weights, as shown in Table 11. The additional criteria for the four models indicate that the best models, in order, are the Squid model, the Branch model, the Fork model, and the existing model. The recommended model must meet the

Table 10. Mandatory criteria scoring

Criteria	MD Unit	Existing	Branch	Fork	Squid
Negative Pressure [kPa]	MD-1	3.080	3.388 ^{AG}	3.428 ^{AG}	3.329 ^{A}
	MD-2	3.108 ^{A}	3.397 ^{AG}	3.421 ^{AG}	3.297 ^{A}
	MD-3	3.070	3.391 ^{AG}	3.431 ^{AG}	3.299 ^{A}
	MD-4	3.191 ^{A}	3.396 ^{AG}	3.419 ^{AG}	3.323 ^{A}
Suction Velocity [m/s]	MD-1	9.36	13.81 ^{AG}	10.92 ^{AG}	15.07 ^{AG}
	MD-2	9.07	14.93 ^{AG}	12.34 ^{AG}	14.91 ^{AG}
	MD-3	9.31	15.02 ^{AG}	12.37 ^{AG}	15.26 ^{AG}
	MD-4	8.57	13.78 ^{AG}	10.90 ^{AG}	15.41 ^{AG}

Note: values followed by ^{A} are capable for Anjasmoro suction-requirement (ΔP_S= 3.094 kPa and $\bar{v}_{SH}$= 10.03 m/s);
values followed by ^{G} are capable for Grobogan suction-requirement (ΔP_S= 3.358 kPa and $\bar{v}_{SH}$= 10.22 m/s).

Table 11. Additional criteria scoring

Criteria	Weight Value	Scaled Scores (0-10)				Product Scores (0-10)			
		Exi.	Branch	Fork	Squid	Exi.	Branch	Fork	Squid
CV for ΔP_{mod}	35%	0.7	10.0	7.0	2.4	0.2	3.5	2.4	0.8
CV for $\bar{v}_{SH}$	35%	3.7	3.1	2.0	10.0	1.3	1.1	0.7	3.5
Total ΔP_{loss}	20%	9.2	9.2	10.0	7.3	1.8	1.8	2.0	1.5
Total local-loss component	10%	10.0	2.6	3.8	10.0	1.0	0.3	0.4	1.0
Accumulative Score		4.4		6.7		5.5			6.8

mandatory criteria and achieve the highest score in the additional criteria. Since the Squid model failed to achieve minimum negative pressure for the seed, therefore, the suction channel system model recommended in this study is the Branch model.

4. CONCLUSION

Optimization of the suction channel system in the existing model was conducted with CFD methods and compared its result against the suction-variable measured of soybean seeds. The Key parameters of seed characteristics for vacuum-type metering performance include require negative pressure and terminal velocity. The require negative pressure for the soybean seeds were determined to be 3.094 kPa (Anjasmoro) and 3.358 kPa (Grobogan), while the terminal velocities achieved were 10.22 m/s (Anjasmoro) and 10.03 m/s (Grobogan). CFD simulation methods were used to predict parameters produced by the existing model with a MAPE score of 11.56% compared to actual values. Three alternative models of the suction channel system were designed: Branch model, Fork model, and Squid model. The negative pressures at the MD produced by existing, Branch, Fork, and Squid model respectively were as follows: 3.112 kPa (CV 1.54%), 3.393 kPa (CV 0.10%), 3.425 kPa (0.15%), and 3.312 kPa (0.43%), while the suction velocity in single seed holes produces are 9.08 m/s (CV 3.44%), 14.39 m/s (CV 4.11%), 11.63 m/s (6.19%), and 15.16 m/s (CV 1.26%). The total pressure-loss that occurs in the system respectively are 118.147 Pa, 117.342 Pa, 108.198 Pa, and 148.335 Pa. Based on the data, the Branch model was selected as the most optimal model compared to others because it could accommodate the required seed parameter for both Anjasmoro and Grobogan variety, ensure uniformity of suction effects on all of the MD unit, and demonstrate channel efficiency.

REFERENCES

Aldio, M.F., Waskito, W., Purwantono, P., & Lapisa, R. (2023). Optimization of impeller blade number in centrifugal pump for crude oil using solidworks flow simulation. *Journal of Engineering Researcher and Lecturer*, ***2***(3), 80-93.

Chakraborty, R., Mandal, U.K., & Barman, R.N. (2016). Pipe flow analysis and its investigation for the selection of water pipeline material using some prominent mcdm methods. *Int. J. Eng. Res. Sci. Technol*, ***5***, 30-41.

da Silva, J.G., Peiter, M.X., Robaina, A.D., Bruning, J., Chaiben Neto, M., & Ferreira, L.D. (2022). Simplified Scobey formula for determining head loss in pressurized pipes. *Brazzilian Journal of Irrigated Agriculture*, ***16***, 31-41. http://dx.doi.org/10.7127/RBAI.V1601254

Hermawan, W., Mandang, T., Sutejo, A., & Saulia, L. (2016). Design and performance of vacuum type seed metering device for precision soybean planter. *ISABE Proceedings; 2016 Agu 9-11*; Lombok, Indonesia.

Hizir, O., Kim, M., Turan, O., Day, A., Incecik, A., & Lee, Y. (2018). Numerical studies on non-linearity of added resistance and ship motions of KVLCC2 in short and long waves. *International Journal of Naval Architecture and Ocean Engineering*, ***11***(1), 143-153. https://doi.org/10.1016/j.ijnaoe.2018.02.015

Ismail, Z.E., Abo El-Magd, A.E., Elbanna, E.B., & Ibrahim, A.A. (2014). Vacuum pressure device as affected by suction tube characteristics. *J.Soil Sci. and Agric. Eng*, ***5***(12), 1635-1644. http://dx.doi.org/10.21608/jssae.2014.49796

Karayel, D., Barut, Z.B., & Özmerzi, A. (2004). Mathematical modelling of vacuum pressure on a precision seeder. *Biosystems Engineering*, ***87***(4), 437-444. http://dx.doi.org/10.1016/j.biosystemseng.2004.01.011

Karayel, D., Güngör, O, & Šarauskis, E. (2022). Estimation of optimum vacuum pressure of air-suction seed-metering device of precision seeders using artificial neural network models. *Agronomy*, ***12***(7), 1600. https://doi.org/10.3390/agronomy12071600

Kurniawardani, R.W., Kristanto, B.A., & Karno, K. (2023). Aplikasi sitokinin dan nanosilika terhadap hasil kedelai (*Glycine max* (L.) Merril) varietas grobogan yang mengalami genangan saat fase awal pembungaan. *Jurnal Agroteknologi Fakultas Pertanian Universitas Muhammadiyah Tapanuli Selatan*, ***8***(1), 200-213.

Lamsal, A. (2023). Analyzing pipe flow scenarios using computational fluid dynamics (CFD). *Int. J. Eng. Appl. Sci. Technol*, ***8***(3), 162-166.

LaNasa, P.J., & Upp, E.L. (2014). *Fluid Flow Measurement* (3rd ed.). Elsevier, Amsterdam, NL: 296 p.

Matouk, A.M., El-Kholy, M.M., Hamam, A.S., & Ewis, T.R. (2005). Aerodynamic characteristics for different varieties of some cereal crops. *J. Agric. Eng. Res*, ***22***(3), 1086-1102.

Moody, L.F., & Princeton, N.J. (1944). Friction factors for pipe flow. *Trans. ASME*, ***66***(November), 671-684.

Mukilan, S. & Vivek, E. (2023). A review of continuity equation for one and three-dimensional flow. *Industrial Engineering Journal*, ***52***(4), 115-119.

Nur, A., Afrianita, R., & Ramli, R.D.T.F. (2019). Effect of pipe diameter changes on the properties of fluid in closed channels using Osborne Reynold Apparatus. *IOP Conf. Series: Materials Science and Engineering*, ***602***, 012058. http://dx.doi.org/10.1088/1757-899X/602/1/012058

Pérez, M.G., & Vakkilainen, E. (2019). A comparison of turbulence models and two and three dimensional meshes for unsteady CFD ash deposition tools. *Fuel*, ***237***, 806-811. http://dx.doi.org/10.1016/j.fuel.2018.10.066

Sagita, D., Hermawan, W., & Setiawan, R.P.A. (2018). Desain dan kinerja mesin pemupuk tipe auger bertenaga traktor tangan untuk tanaman kedelai. *Jurnal Keteknikan Pertanian*, ***6***(2), 187-194. https://doi.org/10.19028/jtep.06.2.187-194

Sun, F., Ji, H., Yang, S., & Li, C. (2023). Numerical investigation on pairing solutions of non-positive displacement pumps and internal gear pump for high-speed design. *Fluids*, ***8***(6), 1-13. https://doi.org/10.3390/fluids8060178

Touloukian, Y.S. (1970). *Thermophysical Properties of Matter*. IFI/Plenum, New York (US): 823 p.

Uribe, J., Saldarriaga, J., & Páez, D. (2015). Effects of the use of Hazen-Williams equation on large WDS planning models. In *World Environmental and Water Resources Congress 2015* (pp. 881-889). http://dx.doi.org/10.1061/9780784479162.083